https://doi.org/10.5194/egusphere-2025-60
Preprint. Discussion started: 31 January 2025

Ion beam instability model for the Mercury upstream waves

Yasuhito Narita[1,*], Daniel Schmid[2,*], and Uwe Motschmann[1,*]

[1]Institut für Theoretische Physik, Technische Universität Braunschweig, Mendelssohnstr. 3, D-38106 Braunschweig, Germany
[2]Space Research Institute, Austrian Academy of Sciences, Schmiedlstr. 6, 8042 Graz, Austria
[*]These authors contributed equally to this work.

Correspondence: Y. Narita (y.narita@tu-braunschweig.de)

Abstract. An analytic model for the ion beam instability is constructed in view of application to the Mercury upstream waves. Our ion beam instability model determines the frequency and the wavenumber by equating the whistler dispersion relation with the beam resonance condition in favor of planetary foreshock wave excitation. By introducing the Doppler shift in the instability frequency, our model can derive the observer-frame relation of the resonance frequency to the beam velocity and the flow speed. The frequency relation serves as a useful diagnostic tool to the Mercury upstream wave studies in the upcoming BepiColombo observations.

1 Introduction

Upstream region of the Mercury bow shock is unique in the plasma physical sense in that the low-frequency electromagnetic waves are excited in the nearly radial interplanetary to the Sun and in a moderate Mach number flow below 10. Diffuse and field-aligned beam and the low-frequency waves are detected by the MESSENGER spacecraft (e.g., Le et al., 2013; Romanelli and DiBraccio, 2021; Glass et al., 2023), mechanism of which is reminiscent of the Earth foreshock formation Naive calculation gives a Parker spiral angle of about 20 degree to the radial direction to the Sun. The MESSENGER magnetic field and the ENLIL model calculation estimate the flow speed is about 350–400 km s^{-1}, which corresponds to an Alfvén Mach number around 6.

Various kinds of low-frequency electromagnetic waves are observed upstream of the Mercury bow shock by the MESSENGER spacecraft such as whistler mode at about 2 Hz (in the spacecraft frame), fast mode wave at about 0.3 Hz (Le et al., 2013), and ion-cyclotron associated with the pick-up protons (Schmid et al., 2022). The lesson from the Earth foreshock studies is that the waves are driven by the shock-reflected, back-streaming ions interacting with the solar wind, and the waves represent the right-hand resonant ion beam instability, also referred to as the component-component instability (Gary, 1993). The pick-up ion cyclotron waves are unique to the extended exospheric region such that the neutral species (atomic hydrogen) is photo-ionized in interplanetary space, and are observed around Mercury (Schmid et al., 2022) as well as Venus and Mars (Delva et al., 2011a, b). Both the foreshock and ion-cyclotron waves exhibit left-hand field rotation about the mean magnetic field in the temporal sense. The right-hand beam resonance undergoes a Doppler shift in the opposite direction to the beam and the

https://doi.org/10.5194/egusphere-2025-60
Preprint. Discussion started: 31 January 2025

wave polarization is reversed into left-hand rotation sense. The pick-up ion cyclotron waves are also observed as a left-handed field rotation sense because the spacecraft frame is virtually the same as the rest frame of pick-up ions.

Here we develop an analytic model of the ion beam instability relevant to the Mercury upstream waves in view of the upcoming arrival of the BepiColombo mission at Mercury (Benkhoff et al., 2021). Our foreshock model is constructed of the dispersion relation of whistler waves and the beam resonance condition. We derive a constraint relation between the frequency (or wavenumber) of the instability, the beam velocity, and the flow speed. The model has a capability to estimate the flow speed if the beam velocity is known or assumed, or vice verse to estimate the beam velocity if the flow speed is known or assumed. In particular, the Mio spacecraft of BepiColombo covers a wide range of radial distance to Mercury up to about 6 planetary radii, which is suited to perform a systematic survey of the Mercury upstream waves with the magnetometer and plasma detectors. Our model serves as a diagnostic tool to determine or constraint the velocities (flow speed and beam velocity) even using the magnetic field data.

2 Resonance frequency estimate

2.1 Problem setup

In the theoretical framework, the beam instability is conveniently analyzed in the rest frame of the bulk plasma. We refer to this frame as the flow frame, comoving with the solar wind. The ion beam is injected into the system at a speed of U_b (the beam direction is taken as positive) along the magnetic field. See the top panel of Fig. 1 for the flow frame setup. In order to interpret the beam instability in the observer frame (representative to the spacecraft frame), the Galilean transformation is introduced with a flow speed U_f (taken as negative, in the opposite direction to the beam). The beam velocity reduces to $U_\mathrm{f} + U_\mathrm{b}$ (see bottom panel of Fig. 1). The observer frame may also be regarded as the shock frame such that the beam velocity is $U_\mathrm{f} + U_\mathrm{b}$ with respect to the bow shock.

2.2 Analysis in the flow frame

The right-hand resonant instability represents an energy and momentum transfer of the beam ions into the electromagnetic waves. The kinetic treatment of the beam instabilities is documented in the framework of linear Vlasov theory by Gary (1993). Single and multi-spacecraft observations in the Earth foreshock region confirm the right-hand resonant instability (Watanabe and Terasawa, 1984; Eastwood et al., 2003; Narita et al., 2003).

The right-hand resonant instability occurs when the low-frequency whistler mode (R+ branch) meets the beam resonance condition. The resonance occurs at a frequency below or around the ion cyclotron frequency. Figure 2 illustrates the dispersion relation diagram of four branches of electromagnetic waves, R+ the right-hand polarized parallel-propagating mode, L+ the left-hand polarized parallel-propagating mode, and R− and L− for the anti-parallel propagation.

The task is to find the crossing frequency between the R+ branch and the resonance condition. The low-frequency part of whistler dispersion relation for parallel propagation in a low-beta plasma (cold plasma) is, by including the effect of Hall

https://doi.org/10.5194/egusphere-2025-60
Preprint. Discussion started: 31 January 2025

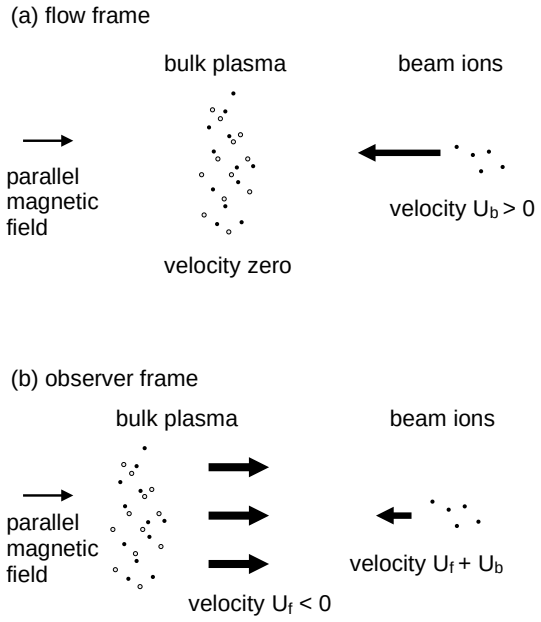

Figure 1. Ion beam injected into the bulk plasma in the flow frame (top) and in the observer frame (bottom).

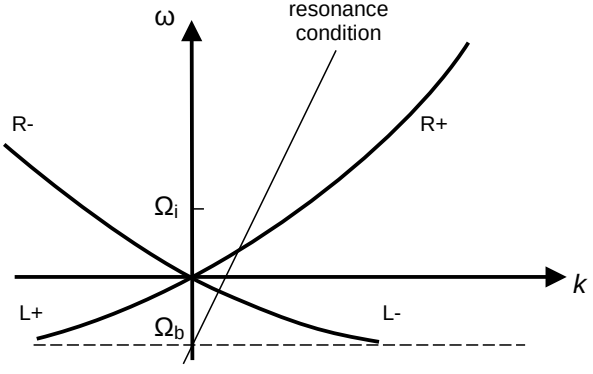

Figure 2. Dispersion relation of the R and L modes with propagation sense, plus for forward and minus for backward propagation with respect to the beam direction. R+ mode (forward whistler) likely undergoes the beam instability because the wave group velocity is in the beam direction. The L- mode resonance with the beam is unlikely because of the opposite propagation direction to the beam (no sufficient time for the energy exchange). The beam cyclotron frequency Ω_b is negative. The ion cyclotron frequency of the bulk plasma is denoted by Ω_i for reference.

current, is obtained after Hasegawa and Uberoi (Eq. 2.24 in 1982) or Gary (Eq. 6.2.5 in 1993) as

$$\frac{\omega}{\Omega_p} \simeq \frac{k_\parallel V_A}{\Omega_p}\left(1+\frac{k_\parallel V_A}{\Omega_p}\right)^{1/2} \quad (1)$$

$$\simeq \frac{k_\parallel V_A}{\Omega_p}+\frac{1}{2}\left(\frac{k_\parallel V_A}{\Omega_p}\right)^2. \quad (2)$$

https://doi.org/10.5194/egusphere-2025-60
Preprint. Discussion started: 31 January 2025

The resonance condition for the beam ions is expressed as

$$\omega - k_{\parallel} U_{\rm b} = -\Omega_{\rm p}. \tag{3}$$

Here ω denotes the wave frequency, k the parallel wavenumber to the mean magnetic field, $V_{\rm A}$ the Alfvén speed, and $\Omega_{\rm p}$ the ion cyclotron frequency for protons.

For an easier theoretical treatment, we normalize the frequency to the ion cyclotron frequency (for the protons) $\Omega_{\rm p}$, and rewrite hereafter the normalized frequency as $\omega/\Omega_{\rm p} \to \omega$. The proton cyclotron frequency is then expressed as unity, $\Omega_{\rm p} \to 1$. The wavenumber is accordingly normalized to the ion inertial length $V_{\rm A}/\Omega_{\rm p}$ and we rewrite the normalized wavenumber as $kV_{\rm A}/\Omega_{\rm p} \to k$. The same normalization applies to the parallel wavenumber. When limiting to the parallel propagation, the whistler dispersion relation (Eq. 1) and the resonance condition are rewritten as

$$\tilde{\omega} = \tilde{k}_{\parallel} + \frac{1}{2}\tilde{k}_{\parallel}^2. \tag{4}$$

and

$$\tilde{\omega} - \tilde{k}_{\parallel}\tilde{U}_{\rm b} = -1, \tag{5}$$

respectively. The beam velocity is normalized to the Alfvén speed.

By eliminating the frequency ω in Eqs. (4) and (5), we obtain the quadratic equation as to the resonance wavenumber,

$$\tilde{k}_{\parallel}^2 - 2(\tilde{U}_{\rm b} - 1)\tilde{k}_{\parallel} + 2 = 0. \tag{6}$$

The roots of Eq. (6) are

$$\tilde{k}_{\parallel} = \tilde{U}_{\rm b} - 1 \pm \sqrt{(\tilde{U}_{\rm b} - \tilde{U}_{-})(\tilde{U}_{\rm b} - \tilde{U}_{+})} \tag{7}$$

$$\tilde{U}_{\pm} = 1 \pm \sqrt{2} \tag{8}$$

For the existence of real-number solution, the beam velocity must satisfy the condition

$$\tilde{U} \geq U_{+} = 1 + \sqrt{2} \tag{9}$$

Interestingly, the threshold value is about $1 + \sqrt{2} \sim 2.4$, which is close to the critical Alfvén Mach number for the shock reflection mechanism. The lower wavenumber solution of Eq. (7) with the minus sign is the resonance wavenumber of interest. The higher wavenumber solution is valid for a lower beam velocity near the "touch point" (Eq. 9), but may not be exact for a higher beam velocity as the parabolic approximation of the whistler mode is no longer valid at higher frequencies. The resonance frequency in the flow frame is derived from Eq. (5) as

$$\omega = \left(\tilde{U}_{\rm b} - 1 - \sqrt{(\tilde{U}_{\rm b} - \tilde{U}_{-})(\tilde{U}_{\rm b} - \tilde{U}_{+})}\right)\tilde{U}_{\rm b} - 1 \tag{10}$$

2.3 Transformation into the observer frame

By introducing the Doppler shift by the bulk flow as $\tilde{k}_{\parallel}\tilde{U}_{\rm f}$ (here $\tilde{U}_{\rm f}$ denotes flow speed in units of the Alfvén speed) in the opposite direction to the beam velocity and transforming the frequency from the flow rest frame into the observer frame, we

https://doi.org/10.5194/egusphere-2025-60
Preprint. Discussion started: 31 January 2025

obtain the resonance frequency $\tilde{\omega}'$ (in units of the proton cyclotron frequency) as

$$\tilde{\omega}' = \tilde{k}_{\parallel}(\tilde{U}_{\rm b} + \tilde{U}_{\rm f}) - 1 \tag{11}$$

$$= \left[(\tilde{U}_{\rm b} - 1) - \sqrt{(\tilde{U}_{\rm b} - \tilde{U}_{-})(\tilde{U}_{\rm b} - \tilde{U}_{+})}\right] \times$$

$$(\tilde{U}_{\rm b} + \tilde{U}_{\rm f}) - 1 \tag{12}$$

Figure 3 displays the dispersion relation and the resonance condition in the comoving frame and the observer frame for $\tilde{U}_{\rm b} = 7$ and $\tilde{U}_{\rm f} = -5$. Whistler wave frequencies are transformed into the negative frequency domain while retaining the wavenumber. The temporal sense of wave field rotation (polarization) changes accordingly from right-hand rotation around the magnetic field into left-hand rotation.

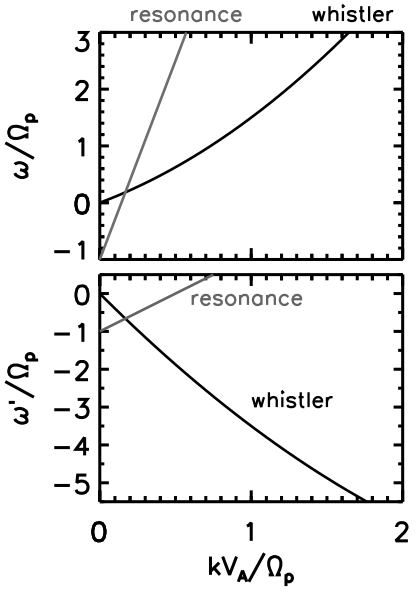

Figure 3. Whistler dispersion relation and beam resonance condition in the comoving frame with the flow (top) and the observer frame standing in the flow for a beam velocity of $U_{\rm b}/V_{\rm A} = 7$ flow speed $U_{\rm f}/V_{\rm A} = -5$ (bottom).

Equation (12) relates the resonance frequency (e.g., peak of the magnetic power spectrum in the spacecraft frame) with the beam velocity and the flow speed. The frequency estimate (Eq. 12) indicates that the ion cyclotron frequency is expected for the beam instability for the pickup ions by substituting the sign-reversed flow speed into beam velocity as $\tilde{U}_{\rm b} = -\tilde{U}_{\rm f}$ (pickup ion cyclotron waves).

3 Velocity estimate

Equation (12) may be regarded as a function of the beam velocity in the flow frame $\tilde{U}_{\rm b}$ and the flow speed $\tilde{U}_{\rm f}$ given that the frequency is known in the observer frame. A useful tool can be developed from Eq. (12). that is, we derive the relation between

https://doi.org/10.5194/egusphere-2025-60
Preprint. Discussion started: 31 January 2025

the beam velocity in the observer frame $\tilde{U}'_{\rm b}$ defined as

$$\tilde{U}'_{\rm b} = \tilde{U}_{\rm b} + \tilde{U}_{\rm f} \tag{13}$$

and the flow speed $\tilde{U}_{\rm f}$ for the resonance frequency $\tilde{\omega}'$. We can derive the expression of $\tilde{U}_{\rm b}$ by transforming Eq. (12) into

$$\frac{\tilde{\omega}'+1}{\tilde{U}'_{\rm b}} - (\tilde{U}_{\rm b}-1) = -\sqrt{(\tilde{U}_{\rm b}-\tilde{U}_-)(\tilde{U}_{\rm b}-\tilde{U}_+)} \tag{14}$$

and squaring Eq. (14) as

$$\left[\frac{\tilde{\omega}'+1}{\tilde{U}'_{\rm b}} - (\tilde{U}_{\rm b}-1)\right]^2 = (\tilde{U}_{\rm b}-\tilde{U}_-)(\tilde{U}_{\rm b}-\tilde{U}_+). \tag{15}$$

Equation (15) is simplified to

$$\tilde{U}_{\rm b} = \frac{\tilde{\omega}'+1}{2\tilde{U}'_{\rm b}} + \frac{\tilde{U}'_{\rm b}}{\tilde{\omega}'+1} + 1. \tag{16}$$

We combine Eq. (16) with Eq. (13), and obtain $\tilde{U}_{\rm f}$ as a function of $\tilde{U}'_{\rm b}$ as

$$\tilde{U}_{\rm f} = -\frac{\tilde{\omega}'+1}{2\tilde{U}'_{\rm b}} + \left(1 - \frac{1}{\tilde{\omega}'+1}\right)\tilde{U}'_{\rm b} - 1. \tag{17}$$

Figure 4 is the graphical representation of Eq. (17) at various values of $\tilde{\omega}'$. Three conditions are imposed for $\tilde{U}_{\rm f}$ and $\tilde{U}'_{\rm b}$: First, the flow is in the negative direction (opposite direction to the beam) in the observer frame, so $\tilde{U}_{\rm f} < 0$. Second, the beam velocity is in the positive direction in the observer frame for the formation of the foreshock region, so $\tilde{U}'_{\rm b} > 0$. Third, the beam resonance must occur, so $\tilde{U}_{\rm b} > \tilde{U}_+$ in the flow frame, which is transformed into $\tilde{U}_{\rm f} < \tilde{U}'_{\rm b} - U_+$ in the observer frame. The velocity diagram shows the relation between the flow speed and the beam velocity if the resonance frequency is set or known. The flow speed has a positive slope to smaller values of beam velocity (typically $\tilde{U}'_{\rm b} < 0.5$), while the slope becomes negative at larger values of beam velocity ($\tilde{U}'_{\rm b} > 0.5$).

One can develop a useful tool from Eq. (17) and the knowledge from the Earth foreshock studies, since the beam velocity is nearly the same as the Alfvén speed in the flow rest frame (Narita et al., 2003). We determine the flow speed as a function of the observer-frame frequency at several representative values of beam velocity (in the observer frame), and plot the diagram in Fig. 5. For the beam velocity of the order of Alfvén speed, $\tilde{U}'_{\rm b}$ or unity or higher, the estimated flow speed is a monotonous function of the observer-frame frequency. The flow velocity increases more rapidly at higher frequencies (typically $\tilde{\omega}' > 0.4$). Figure 5 gives us a range of of the estimated flow speed if the range of beam velocity is set.

4 Concluding remarks

Our ion beam instability model determines the resonance frequency and wavenumber by equating the low-frequency whistler dispersion relation with the beam resonance condition in favor of planetary foreshock wave excitation. The resonance is of right-hand type in favor of $R+$ mode (whistler branch), and occurs at a beam velocity of at least $\tilde{U}_{\rm b} = 1+\sqrt{2} \sim 2.4$ in the flow

https://doi.org/10.5194/egusphere-2025-60
Preprint. Discussion started: 31 January 2025

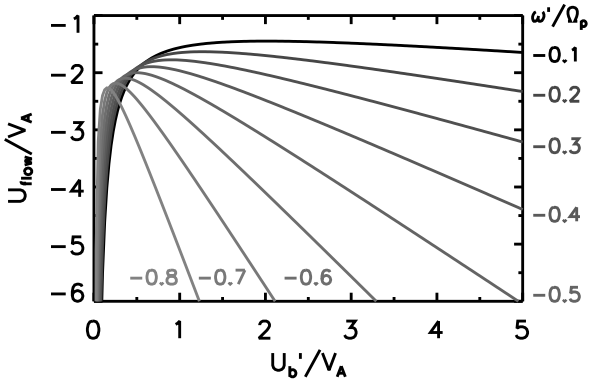

Figure 4. Velocity diagram showing the flow speed (normalized to the Alfvén speed) $U_{\rm f}/V_{\rm A}$ as a function of the beam velocity (also normalized to the Alfvén speed) in the observer frame $\tilde{U}'_{\rm b}/V_{\rm A}$ at different values of the resonance frequency (normalized to the proton cyclotron frequency) in the observer frame $\tilde{\omega}'/\Omega_{\rm p}$.

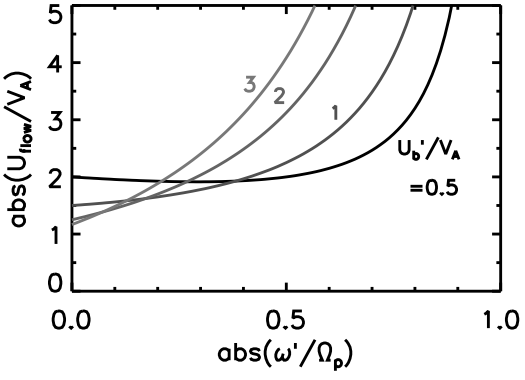

Figure 5. Flow speed diagram as a function of the resonance frequency in the observer frame at different beam velocities. Absolute values of the frequency and the flow speed are used in the plot.

rest frame. The instability condition is likely satisfied in the near-Mercury solar wind as the Mach number is mostly above 4 after the MESSENGER observation and the ENLIL calculation (Winslow et al., 2013). It is interesting to note that the critical beam velocity $\tilde{U}_{\rm b} \sim 2.4$ roughly coincides with the critical Alfvén Mach number for the specular reflection at the collisionless shocks (which is about 2.7).

Our model is capable of predicting the wavelength and the frequency for the beam instability for the given set of beam velocity and flow speed. Here is an example. For a beam velocity of $\tilde{U}'_{\rm b} = 1$ in the observer frame and a flow Mach number of 6 in the opposite direction to the beam $\tilde{U}_{\rm f} = -6$ (e.g., Winslow et al., 2013), we obtain the beam velocity in the flow frame as $\tilde{U}_{\rm b} = \tilde{U}_{\rm b} + \tilde{U}_{\rm f} = 7$. The resonance wavenumber is estimated as $k_{\parallel} V_{\rm A}/\Omega_{\rm p} \simeq 0.17$ (Eq. 7) and the frequency as $\omega'/\Omega_{\rm p} \simeq -0.83$ (Eq. 11). By referring to the magnetic field statistics of about 20 nT (Romanelli and DiBraccio, 2021) and the ion density of

https://doi.org/10.5194/egusphere-2025-60
Preprint. Discussion started: 31 January 2025

about 40 cm^{-3} (Winslow et al., 2013), we obtain an Alfvén speed of $V_A \simeq 70$ km s^{-1} and an ion inertial length of $V_A/\Omega_p \simeq 3.7$ km rad^{-1}. The resonance wavelength is thus estimated as 3.5 km and the frequency as 2.5 s^{-1}, which is well within the sampling rate of the fluxgate magnetometer on-board the BepiColombo Mio spacecraft with 128 Hz for the burst mode or H mode, and 8 Hz for the normal mode or M1 mode (Baumjohann et al., 2020).

Our model is developed for a one-dimensional setup, that is, the beam velocity, the flow, and the wave propagation are assumed to be all aligned with the mean magnetic field. Even though such an aligned situation is most likely realized in the Mercury upstream region as the Parker spiral angle is the smallest (most radial) of all the solar system planets, our model may be upgraded to a weakly misaligned wave system (like the effect of inclination of the mean magnetic field to the flow direction or a moderately oblique propagation angle to the mean magnetic field) by projecting the misaligned system onto our one-dimensional treatment.

Code and data availability. No codes or data are used in this work.

Author contributions. All authors listed have made a substantial, direct, and intellectual contribution to the work and approved it for publication.

Competing interests. Conflict of Interest: The authors declare that the research was conducted in the absence of any commercial or financial relationships that could be construed as a potential conflict of interest.

Acknowledgements. We acknowledge the funding assist by German Science Foundation under project number 535057280.

https://doi.org/10.5194/egusphere-2025-60
Preprint. Discussion started: 31 January 2025

References

Baumjohann, W., Matsuoka, A., Narita, Y., Magnes, W., Heyner, D., Glassmeier, K.-H., Nakamura, R., Fischer, D., Plaschke, F., Volwerk, M., Zhang, T L., Auster, H.-U., Richter, I., Balogh, A., Carr, C. M., Dougherty, M., Horbury, T. S., Tsunakawa, H., Matsushima, M., Shinohara, M., Shibuya, H., Nakagawa, T., Hoshino, M., Tanaka, Y., Anderson, B. J., Russell, C. T., Motschmann, U., Takahashi, F., and Fujimoto, A., The BepiColombo–Mio magnetometer en route to Mercury, Space Sci. Rev., 216, 125, 2020. https://doi.org/10.1007/s11214-020-00754-y

Benkhoff, J., Murakami, G., Baumjohann, W., Besse, S., Bunce, E., Casale, M., Cremosese, G., Glassmeier, K.-H., Hayakawa, H., Heyner, D., Hiesinger, H., Huovelin, J., Hussmann, H., Iafolla, V., Iess, L., Kasaba, Y., Kobayashi, M., Milillo, A., Mitrofanov, I. G., Montagnon, E., Novara, M., Orsini, S., Quemerais E., Reininghaus, U., Saito, Y., Santoli, F., Stramaccioni, D., Sutherland, O., Thomas, N., Yoshikawa, I., and Zender, J., BepiColombo – Mission Overview and Science Goals. Space Sci. Rev., 217, 90, 2021. https://doi.org/10.1007/s11214-021-00861-4

Delva, M., Mazelle, C., Bertucci, C., Volwerk, M., Vörös, Z., and Zhang, T. L., Proton cyclotron wave generation mechanisms upstream of Venus. J. Geophys. Res. Space Physics, 116, A02318, 2011. https://doi.org/10.1029/2010ja015826

Delva, M., Mazelle, C., and César, B., Upstream Ion Cyclotron Waves at Venus and Mars, Space Sci. Rev., 162, 5–24, 2011. https://doi.org/10.1007/s11214-011-9828-2

Eastwood, J. P., Balogh, A., Lucek, E. A., Mazelle, C., and Dandouras, I., On the existence of Alfvén waves in the terrestrial foreshock, Ann. Geophys., 21, 1457–1465, 2003. https://doi.org/10.5194/angeo-21-1457-2003

Gary, S. P., Theory of Space Plasma Microinstabilities, Cambridge University Press, 1993. https://doi.org/10.1017/CBO9780511551512

Glass, A. N., Tracy, P. J., Raines, J. M., Jia, X., Romanelli, N., and DiBraccio, G. A. Characterization of Foreshock Plasma Populations at Mercury, J. Geophys. Res. Space Physics, 128, e2022JA031111, 2023. https://doi.org/10.1029/2022JA031111

Hasegawa, A., and Uberoi, C., The Alfvén wave, DOE Critical Review Series, DOE/TIC-11197, Technical Information Center, U.S. Department of Energy, 1982. https://doi.org/10.2172/5259641

Le, G., Chi, P. J., Blanco-Cano, X., Boardsen, S., Slavin, J. A., Anderson, B. J., and Korth, H., Upstream ultra-low frequency waves in Mercury's foreshock region: MESSENGER magnetic field observations, J. Geophys. Res. Space Physics, 118, 2809–2823, 2013. https://doi.org/10.1002/jgra.50342

Narita, Y., Glassmeier, K.-H., Schäfer, S., Motschmann, U., Sauer, K., Dandouras, I., Fornaçon, K.-H., Georgescu, E., and Rème, H., Dispersion analysis of ULF waves in the foreshock using cluster data and the wave telescope technique, Geophys. Res. Lett., 30, 1710, 2003. https://doi.org/2003GL017432

Narita, Y., Kinetic extension of critical balance to whistler turbulence, Astrophys. J., 831, 83, 2016. https://doi.org/0.3847/0004-637X/831/1/83

Romanelli, N., and DiBraccio, G. A., Occurrence rate of ultra-low frequency waves in the foreshock of Mercury increases with heliocentric distance, Nature Comm., 12, 6748, 2021. ttps://doi.org/10.1038/s41467-021-26344-2

Schmid, D. Lammer, H., Plaschke, F., Vorburger, A., Erkaev, N. V., Wurz, P., Narita, Y. Volwerk, M., Baumjohann, W., and Anderson, B. J., Magnetic evidence for an extended hydrogen exosphere at Mercury, J. Geophys. Res. Planets, 127, e2022JE007462, 2022. https://doi.org/10.1029/2022JE007462

Watanabe, Y., and Terasawa, T., On the excitation mechanism of the low-frequency upstream waves, J. Geophys. Res., 89, 6623–6630, 1984. https://doi.org/10.1029/JA089iA08p06623

https://doi.org/10.5194/egusphere-2025-60
Preprint. Discussion started: 31 January 2025

190 Winslow, R. M., Anderson, B. J., Johnson, C. L., Slavin, J. A., Korth, H., Purucker, M. E., Baker, D. N., Solomon, S. C., Mercury's magnetopause and bow shock from MESSENGER Magnetometer observations, J. Geophys. Res. Space Physics, 118, 2213–2227, 2013. https://doi.org/10.1002/jgra.50237